Joint Pathology Center
Veterinary Pathology Services

WEDNESDAY SLIDE CONFERENCE 2024-2025

Conference #6 — 18 September 2024

CASE I:

Signalment:
12.5 month old R672C heterozygous rat (Sprague-Dawley background)

History:
This R672C heterozygous rat was reported for bilateral hindlimb weakness. On exam, the rat was bright, alert, responsive, groomed, and had a BCS of 4/5. He was active and able to move around the cage using the fore limbs but dragged the hind limbs, which had severe proprioceptive deficits (right more severe than left). The withdrawal reflex was present but diminished in both hind limbs. The tail was also limp, and the rat was unable to freely move its tail (the tail dropped after picking it up and letting it go). There is no experimental history for this rat. The phenotype may include limb contracture, although the research group has not observed this phenotype.

Gross Pathology:
The rat is in fair postmortem condition and has a body condition score of 5/5 with substantial subcutaneous and visceral adipose stores. Within the abdomen, the spleen is markedly enlarged. There is a 5 mm x 1 mm green area on the serosal surface of the spleen that does not extend into the parenchyma. The kidneys have bilateral multifocal to coalescing green-tan foci, ranging in size from ~1mm to 5mm. Some of the foci are slightly raised; on cut section, they extend into the renal cortex and are semi-firm. The left and right renal cortex and medulla are moderately diffusely dark red in

Figure 1-1. Kidney, rat. The kidneys have bilateral slightly raised tan to green nodules extending into the cortex. (*Photo courtesy of:* University of Washington Veterinary Diagnostic Lab and Comparative Pathology Program, Department of Comparative Medicine, The Comparative Pathology Program (CPP) | Department of Comparative Medicine (washington.edu)

color with minimal corticomedullary distinction. The liver is mildly increased in size and is mottled red pink. There is a 1.5 cm x 1 cm green tubular soft tissue structure at the level of the ventral left lateral liver lobe. There is mild segmental reddening of the small intestine. Upon removal of the gastrointestinal tract, there are multiple 3-5 mm green soft tissue semi-firm structures within the visceral adipose tissue.

The vertebral column is removed from the level of the third lumbar vertebrae to the third sacral vertebrae. On cross section, within the vertebral canal, there is brown-green caseous material surrounding the spinal cord. Within

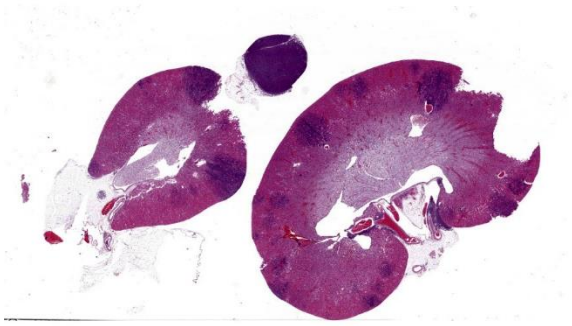

Figure 1-2. Kidney, adrenal gland, rat. The adrenal gland is diffusely effaced, and the renal cortex is multifocally infiltrated by a round cell neoplasm. (HE, 4X)

the bone marrow of the femur, there is green caseous material that exudes on cut section.

The lungs are mottled light red to pink. The heart is mildly enlarged. Within the mediastinum, there are multiple, 5mm-7mm green soft tissue structures. Within the ventral neck, structures of the same appearance are observed, approximately at the level of the cervical lymph nodes. There are no other significant findings.

Laboratory Results:
Mediastinal mass culture: No growth on initial plate media. Leuconostoc pseudomesenteroides from enrichment broth only – presume contaminant.

Microscopic Description:
Kidney: Expanding the interstitium and separating the tubules, there is an unencapsulated and infiltrative neoplasm characterized by sheets of round cells with mild to moderate cytoplasm in a scant preexisting fibrovascular stroma. Nuclei are circular to ovoid and occasionally reniform, with a single distinct nucleolus. In some cells, there is an eccentric nucleus with eosinophilic cytoplasm. Cell borders are generally distinct. There is moderate anisocytosis and anisokaryosis. Mitoses are frequent. Many tubular epithelial cells contain intracytoplasmic eosinophilic droplets of varying size, up to 20 microns in diameter. The adrenal gland is effaced by similar neoplastic cells.

The round cell neoplasm also affects the following organs: bone marrow, head (Harderian gland, nasal cavity, salivary gland), meninges, lung, liver, kidney, lymph node, pancreas, spleen, submucosa of the bladder, fat, epaxial skeletal muscle, and nerve roots

Contributor's Morphologic Diagnoses:
1. Multiorgan hematopoietic neoplasm.
2. Renal tubular epithelium: Intracytoplasmic hyaline droplets.

Contributor's Comment:
The neoplasm in this rat is most consistent with a hematopoietic neoplasm. Hematopoietic neoplasms reported in rats include lymphoma, granulocytic leukemia (myeloid sarcoma), and histiocytic sarcoma.[2] Hematopoietic neoplasms in general are much less common in the rat compared to the mouse.[2] In one report, lymphoma had an approximately 1.5% incidence in the Sprague Dawley rat, of which large granular lymphocyte lymphoma (or mononuclear leukemia) was most common, and granulocytic leukemia had a 0.1-0.3% incidence.[2] Granulocytic leukemia more often involves in the kidney in the rat in addition to other organs such as the liver, spleen and bone marrow, and cells with ring shaped nuclei or large, blastic cells may be seen. [2,3] Histiocytic sarcoma is the most common nonlymphoid hematopoietic neoplasm reported in the rat and is recognized as an age related neoplasm in the Sprague Dawley and other strains of rat.[2, 5] This neoplasm has been reported to have an incidence of approximately 1% in Sprague Dawley rats, usually affects rats over 12 months of age, and most commonly affects the lung and liver.[2,3] Other authors have

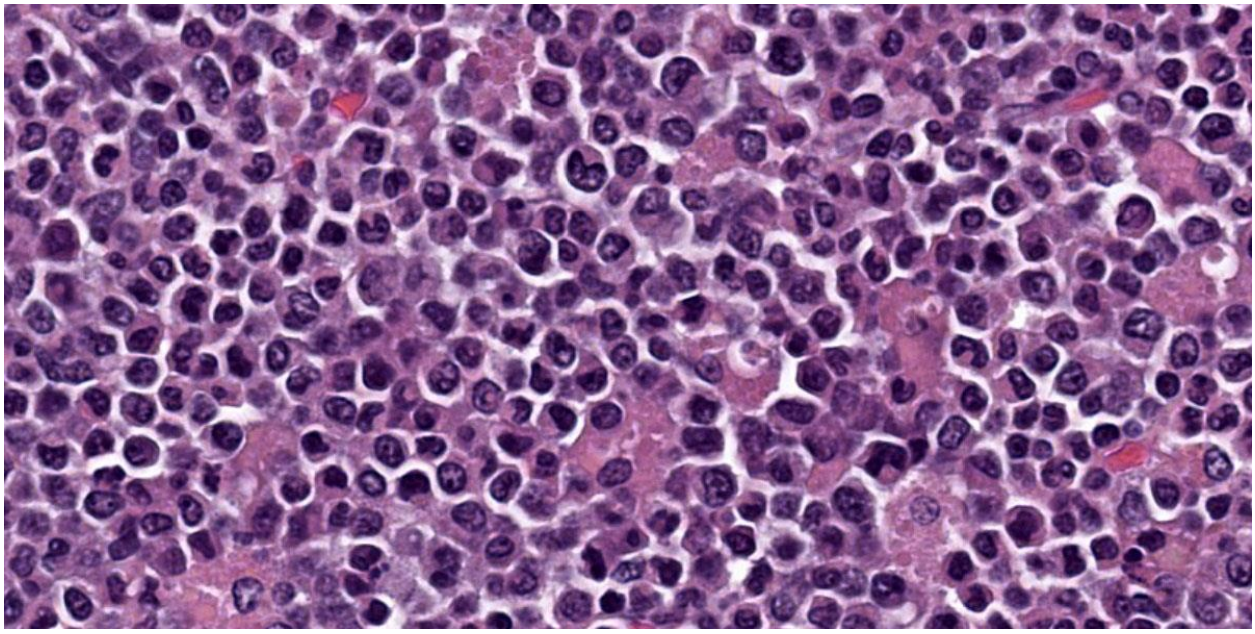

Figure 1-3. Adrenal gland, rat. Neoplastic rounds cells have a round to indented nucleus and there is a high mitotic count. (HE, 900X)

described the neoplasm affecting hematopoietic organs including bone marrow, spleen and lymph nodes in the rat.[5] Histiocytic sarcoma arises from histiocytes although the exact origin of the histiocytic cells remains uncertain.[3] These cells arise from the mononuclear-phagocyte system lineage, and include promonocytes, monocytes, tissue histiocytes, and macrophages.[3] Histologically, the neoplasm may have a granulomatous or sarcomatous appearance or present as sheets of round cells, and multinucleated giant cells are frequently observed.[4] This neoplasm does not have a granulomatous or sarcomatous appearance, and multinucleated giant cells are not observed in the present case.

In the rodent, histiocytic sarcoma and occasionally other hematopoietic neoplasms may be associated with intracytoplasmic round eosinophilic droplets containing lysozyme in the tubular epithelial cells.[3] In one study, 74 of 77 Sprague Dawley rats with
histiocytic sarcoma had renal hyaline droplet accumulation.[3] The presence of this feature in rodents with histiocytic sarcoma appears to correlate with tumor burden and is likely associated with overproduction of endogenous protein by the neoplastic cells.[3] Other differentials for eosinophilic droplets within the proximal tubular epithelium of the rat include α-2u globulin nephropathy.[3] In the mouse and rat, chronic progressive nephropathy and other neoplasms may also be associated with hyaline droplet formation.[1]

Immunohistochemistry is helpful to confirm the diagnosis of hematopoietic neoplasms. Macrophages may require a panel of antibodies for diagnosis due to varying phenotypes in different tissue environments.[6] Common antibodies used in the diagnosis of histiocytic sarcoma in the rat include CD68 (ED-1) and lysozyme, among others.[5,6] Lysozyme is also reported in the diagnosis of granulocytic leukemia, in addition to myeloperoxidase (MPO).[6] Antibodies useful in the diagnosis of lymphoma in the rat have also been reported.[6] None of these antibodies,

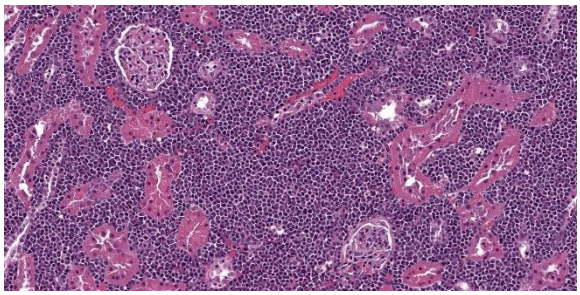

Figure 1-4. Kidney, rat. Similar neoplastic cells infiltrate the renal cortex. (HE, 190X)

unfortunately, are optimized in our laboratory for the rat.

Contributing Institution:
University of Washington Veterinary Diagnostic Lab and Comparative Pathology Program

Department of Comparative Medicine

The Comparative Pathology Program (CPP) | Department of Comparative Medicine (washington.edu)

JPC Diagnoses:
1. Kidney and lymph node: Hematopoietic sarcoma.
2. Renal tubular epithelium: Intracytoplasmic hyaline droplets.

JPC Comment:
This week's moderator was Dr. Michael Eckhaus from the National Institutes of Health who provided a lab-animal centric conference for participants.

In this first case, conference participants debated the exact origin of neoplastic cells, as the reniform nuclei may be seen in neoplasms of both histiocytic and granulocytic origin. To better characterize these neoplastic cells, we ran typical round cell immmunomarkers (IBA1, CD3, CD20, PAX5, MUM1, and lysozyme), all of which were negative. Unfortunately CD34 and myeloperoxidase, markers that should stain cells of myeloid origin were immunonegative as well. The gross description of the greenish nodules (figure 1-1) hints at a granulocytic (myeloid) leukemia origin, but we were unable to confirm their identity with more objective means. Based on the HE appearance, we ultimately agreed with the contributor on the morphologic diagnosis.

This case is also a nice example of hyaline droplets in the kidney of a rat (figure 1-5). While most participants recognized the hyaline droplets and associated them with a diagnosis of histiocytic sarcoma in this case, the droplets (and neoplastic cells) did not stain for lysozyme. Alpha-2u globulin nephropathy is another consideration for these droplets, though this animal did not have any history of chemical exposure. In Alpha-2u globulin nephropathy, hyaline droplets represent secondary lysosomes containing alpha-2u-globulin bound to a variety of chemicals and/or their metabolites with the complex being resistant to proteolytic degradation which promotes accumulation within the cytoplasm.[7] Hyaline droplets are also a normal finding in male rats, albeit at a low background level far less than that seen in this case.

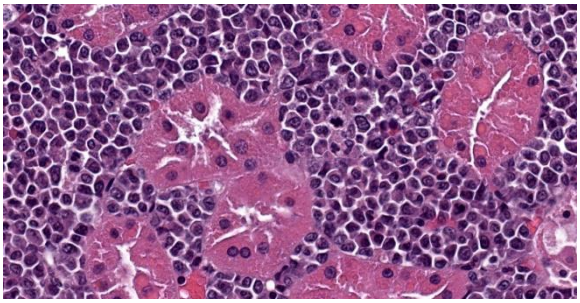

Figure 1-5. Kidney, rat. Proximal convoluted tubular epithelium contains numerous intracytoplasmic protein droplets. (HE, 900X)

References:

1. Decker JH, Dochterman LW, Niquette AL, et al. Association of Renal Tubular Hyaline Droplets with Lymphoma in CD-1 Mice. *Toxicol Pathol*. 2012; 40: 651-655.
2. Frith CH. Morphologic Classification and Incidence of Hematopoietic Neoplasms in the Sprague-Dawley Rat. *Toxicol Pathol.* 1998; 16: 451-457.
3. Frith CH, Ward JM, and Chandra M. The morphology, immunohistochemistry, and incidence of hematopoietic neoplasms in mice and rats. *Toxicol Pathol*. 1993; 21:206-218.
4. Hard GC and Snowden RT. Hyaline Droplet Accumulation in Rodent Kidney Proximal Tubules: An Association with Histiocytic Sarcoma. *Toxicol Pathol*. 1991; 19: 88-97.
5. Ogasawara H, Mitsumori K, Onodera, H et al. Spontaneous Histiocytic Sarcoma with Possible Origin from the Bone Marrow and Lymph Node in Donryu and F-344 Rats. *Toxicol Pathol*. 1993; 21: 63-70.
6. Rehg JE, Bush D, and Ward JM. The Utility of Immunohistochemistry for the Identification of Hematopoietic and Lymphoid Cells in Normal Tissues and Interpretation of Proliferative and Inflammatory Lesions of Mice and Rats. *Toxicol Pathol*. 2012; 40: 345-374.
7. Swenberg JA, Short B, Borghoff S, Strasser J, Charbonneau M. The comparative pathobiology of alpha 2u-globulin nephropathy. *Toxicol Appl Pharmacol*. 1989 Jan;97(1):35-46.

CASE II:

Signalment:

12-week-old male ABCA4 -/- mouse.

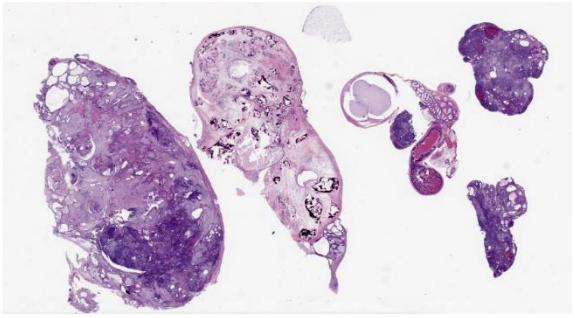

Figure 2-1. Caudal abdominal mass, mouse. Multiple sections of a caudal abdominal mass adjacent to the seminal vesicles is submitted for examination. (HE, 5X)

History:

A 12-week-old male ABCA4 -/- mouse was presented for routine necropsy; no associated clinical signs were reported.

All procedures performed on animals were in accordance with regulations and established guidelines and were reviewed and approved by an Institutional Animal Care and Use Committee or through an ethical review process.

Gross Pathology:

Expanding the abdominal cavity and displacing abdominal organs were multiple variably sized irregular masses. The masses were pale tan and smooth.

Microscopic Description:

Mass: Loosely associated with the seminal vesicle is a well-demarcated, unencapsulated, multinodular neoplastic mass. The densely cellular to cystic neoplasm is composed of variably differentiated neoplastic cells from three, depending on the section, germ cell layers and multiple tissue types. Ectodermal tissue includes neural tissue, including neurons and glial cells, surrounded by neuropil, and multifocal nests and cysts of squamous epithelium with variable keratinization. In addition, fusiform cells arranged in rosettes, suggestive of neuroendocrine origin, are scattered

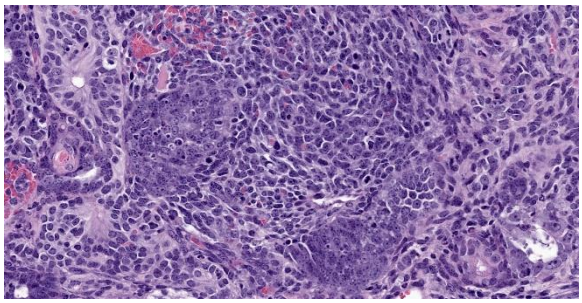

Figure 2-2. Caudal abdominal mass, mouse. Scattered throughout the mass is a population of poorly differentiated pluripotent cells. (HE, 350X)

throughout the mass. Endodermal tissue includes multifocal variably sized tubules lined by cuboidal to columnar epithelial cells. Columnar epithelial cells are often pseudostratified and have apical cilia (respiratory epithelium); goblet cells are interspersed. Mesodermal tissue includes multifocal bundles of smooth muscle, multifocal foci of osteocytes embedded in eosinophilic osteoid and depending on the section, foci of calcified bone, adipose tissue, and rare aggregates of chondrocytes embedded in chondroid matrix (consistent with cartilage). On average, there are less than 1 mitotic figures per high power field.

Contributor's Morphologic Diagnosis:
Abdominal mass, teratoma.

Contributor's Comment:
Although uncommon in domestic animals, teratomas have been reported in a wide variety of veterinary species. In domestic animals teratomas of the testis have been occasionally reported in foals[7], while in laboratory animals, teratomas have been reported in mice, rats, ferrets, and non-human primates.[3,4,8,13] In certain inbred mouse strains, notably 129 mice and its substrains, teratomas have been recognized in the veterinary literature as spontaneous neoplasms since 1954.[4,12] In the 129-mouse strain, a *ter* mutation is responsible for the increase in teratoma incidence.[4]

Thought to arise from multipotent germ cells, teratomas have been reported in multiple tissues including brain, adrenal glands, gonads, uterus.[2,4,10,13] In the nervous system, suprasellar germ cell tumors, like teratomas are most commonly identified on midline.[2] The presence of tissue derived from more than one germinal layer, ectoderm, endoderm, and/or mesoderm, is a requirement for a teratoma diagnosis.[1,7,11] The presence of two or more germinal layers is a result of the initial somatic differentiation of germ cells, giving rise to a variety of tissues that can be present in these tumors.[11] In females, ovarian teratomas are considered parthenogenic tumors, as they are thought to arise from a single germ cell, which has undergone an initial round of meiotic division, but not a second.[11]

Macroscopically, teratomas can be solid and/or cystic, and occasionally contain obvious hair, bone, or teeth.[7,11] Histologically, numerous tissue types have been reported to be components of teratomas, and these various tissue elements can be either mature or immature.[6] In this case, nervous tissues, squamous epithelium, respiratory epithelium, adipose

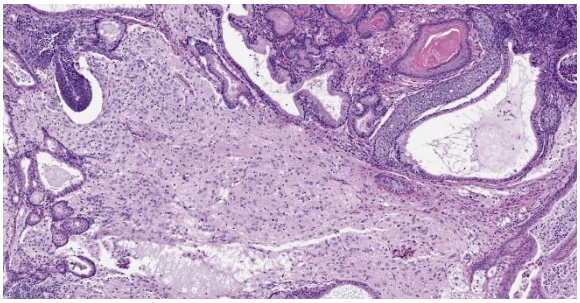

Figure 2-3. Caudal abdominal mass, mouse. Ectodermal tissue in this field includes well-differentiated neuropil with abundant glia, cysts of keratinizing epithelial cells, and cysts lined by ependymal cells. Mesenchymal tissues include well-differentiated cartilage, and several cysts lined by ciliated respiratory epithelium. (HE, 90X).

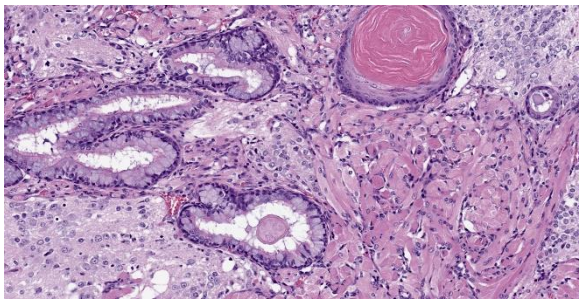

Figure 2-4. Caudal abdominal mass, mouse. Endodermal tissue in this field includes numerous cysts lined by enterocytes and goblet cells adjacent to disorganized bundles of smooth muscle (mesodermal). (HE, 90X)

tissue, smooth muscle, bone, and cartilage were all present. Nervous tissue, adipose tissue, and respiratory epithelium are commonly found in teratomas.[7]

Benign teratomas are characterized by well differentiated tissue, with no significant hemorrhage or necrosis.[5] Benign teratomas do not invade surrounding tissue and do not metastasize, while malignant teratomas have evidence of local invasion and/or metastasize.[4,5] At gross necropsy of this ABCA4-/- mouse, multiple masses were scattered throughout the abdomen, consistent with carcinomatosis and malignant behavior. Although standard histologic evaluation of teratomas is likely sufficient for diagnosis, immunohistochemistry can be employed to highlight the different tissue types.

Contributing Institution:
Pfizer Research and Development
455 Eastern Point Rd.,
Groton, CT 06340
www.pfizer.com

JPC Diagnosis:
Caudal abdominal mass: Teratoma

JPC Comment:
Teratomas are a regular submission to the WSC (Conference 1, Case 4, 2023-2024 and Conference 16, Case 2, 2020-2021). Case 2 is a classic teratoma with a wide array of recognizable tissues from multiple germ cell layers (figures 2-3 through 2-5. Although not needed for this case, histo- and immunohistochemical stains can assist in the recognition of certain tissues. In this case, cartilage is nicely outlined by an Alcian blue pH 1.0 while PAS highlights mucus within goblet cells and basement membranes adjacent to epithelial tissues. Conference participants noted ancillary features such as an inflammatory exudate (sans bacteria) within the cysts lined by respiratory epithelium (however, we refrained from diagnosis any type of pneumonia in this case). There was brief discussion of the potential behavior of this teratoma based on its morphology; participants agreed that the morphology appeared more "benign" than the history provided by the contributor. Other recent WSC submissions have featured more clear examples of malignant behavior with invasion of adjacent issues

Case reports of teratomas have recently been published in cats and in birds.[9,14] Extragonadal teratomas are unusual in domestic animals; two recent feline cases dealt with oropharyngeal teratomas.[14] Similar to human congenital oropharyngeal teratomas, affected cats were young and had masses near the sphenoid bone consistent with an origin from Rathke's

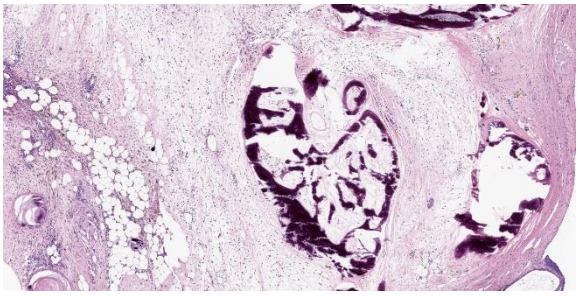

Figure 2-5. Caudal abdominal mass, mouse: Mesodermal tissue in this field includes bone and fat. (HE, 90X).

pouch. In contrast, a coelomic teratoma was described in a 26 year-old eclectus parrot. [9] Despite the mass being well-differentiated, the large size was sufficient to induce increased respiratory effort, lethargy, regurgitation, and adhesions to multiple organs. Although the mass was successfully resected, the bird decompensated and died after surgery.[9] This is an effective reminder that benign neoplasms can still have significant effects on morbidity and mortality.

References:

1. Agnew DW, MacLachlan NJ. Tumors of the Genital Systems. In: Meuten DJ, ed. *Tumors in Domestic Animals, 5th ed*. 2017; Ames, IA, John Wiley & Sons, Inc., p. 689-722.
2. Cantile C, Youssef S. Nervous System, In: Maxie MG, ed. *Jubb Kennedy and Palmer's Pathology of Domestic Animals, 6th ed*. 2016; St. Louis MO, Elsevier Press, vol 1, p. 404.
3. Cline JM, Wood CE, Vidal JD, et al. Selected Background Findings in Interpretation of Common Lesions in the Female Reproductive System in Macaques. *J Toxicol Pathol* 2008; 142S-163S.
4. Creasy D, Bube A, de Rijk E, et al. Proliferative and Nonproliferative Lesions of the Rat and Mouse Male Reproductive System, *J Toxicol Pathol* 2012; 40: 40S-121S.
5. Dixon D, Alison R, Bac U, et al. Nonproliferative and Proliferative Lesions of the Rat and Mouse Female Reproductive System. *J Toxicol Pathol* 2014; 27 (3 & 4 Supplemental):1S-107S.
6. Epstein JI, Lotan TL. The Lower Urinary Tract and Male Genital System. In: Kumar V et al. ed. *Robbins and Cotran Pathologic Basis of Disease.* 9th ed. 2015; Philadelphia, PA, Elsevier Saunders. p. 959-990.
7. Foster RA. Male Genital System, In: Maxie MG, ed. *Jubb Kennedy and Palmer's Pathology of Domestic Animals, 6th ed*. 2016; St. Louis MO, Elsevier Press, vol 3, p. 465-510.
8. Kirejczyk S, Pinelli C, Gonzalez O, et al. Urogenital Lesions in Nonhuman Primates at Two National Primate Research Centers. *Vet Pathol*. 2021 January; 58(1): 147-160.
9. Mayer CC, Richard JN, Lin CM, Conrado FO, Hahn S, Graham JE, Bercier M. Intracoelomic Teratoma in an Eclectus Parrot (Eclectus roratus). *J Avian Med* Surg. 2021 Jul;35(2):217-226.
10. Ogata K, Masahiko K, Miyata K et al. Well-Differentiated Teratoma in a Mouse Uterus. *J Toxicol Pathol* 2011; 39: 901-904.
11. Schlafer DH and Foster RA. Female Genital System, In: Maxie MG, ed. *Jubb Kennedy and Palmer's Pathology of Domestic Animals, 6th ed*. 2016; St. Louis MO, Elsevier Press, vol 3, p. 359-464.
12. Stevens LC and Little CC. Spontaneous Testicular Teratomas in and Inbred Strain of Mice. *Proc Natl Acad Sci USA.* 1954 Nov; 40(11): 1080-1087.
13. Williams BH, Yantis LD, Craig SL, et al. Adrenal Teratoma in Four Domestic Ferrets (*Mustela purorius furo*). *Vet Pathol* 2001; 38: 328-331.
14. Yuzbasioglu-Ozturk G, Gulcubuk A, Ozturk-Gurgen H, Demirutku A, Akcasiz ZN, Ozkul S. An unusual case of oropharyngeal mature teratoma in a kitten. *Iran J Vet Res*. 2023;24(4):365-368.

CASE III:

Signalment:

23.5 year old female rhesus macaque (*Macaca mulatta*).

History:

This monkey had acute, bilateral hind limb paralysis with intact patellar reflexes and an otherwise normal neurologic exam and was euthanized due to welfare concerns. Two years

Figure 3-1. Ovaries and uterus, rhesus macaque. The left ovary (top) is expanded by a 4.5 x 4 x 4 cm mottled tan to red encapsulated mass. The uterus (middle), and right ovary (bottom). (*Photo courtesy of:* Wake Forest School of Medicine, Department of Pathology, Section on Comparative Medicine,www.wakehealth.edu).

prior to euthanasia an adenocarcinoma was excised from the cecum.

Gross Pathology:
A 4.5 x 4 x 4 cm, 34.68 g tan to red firm mass and effaced the left ovary. On sectioned surface the neoplasm was mottled tan to pink with small, scattered areas of central hemorrhage and necrosis. The L1-L2 intervertebral disc had small hemorrhages and was friable.

Microscopic Description:
(The submitted slide includes portions of the ovarian tumor, oviduct, uterus, and ventral segment of the vertebral body.) Left ovary: An encapsulated epithelial neoplasm expands and effaces the entire ovary. The neoplastic cells are arranged in streams, nests and acini on a dense, highly cellular fibrovascular stroma. The cells are closely-spaced, and vary from columnar where forming acini, to spindle-shaped when in streams and along the capsule margin. They have eosinophilic cytoplasm and central nuclei with finely-stippled chromatin and single prominent nucleoli. Many cells are multinucleated, with up to four nuclei. Mitotic figures average 1 per 40x field, with rare bizarre forms. The capsule is invaded by neoplastic cells forming single-file rows. Central necrosis is prominent, and many neutrophils and lymphocytes are scattered throughout. Small rafts of neoplastic cells are present within the adhered myometrium, and in the lumina of uterine vessels.

Vertebra – L2: (ventral aspect of the vertebral body): Approximately 70% of the marrow cavity is effaced by neoplastic cells similar to those described for the ovary, interspersed with pale eosinophilic necrotic cellular debris and blood. Neoplastic acini invade into and through the vetebral cortical bone. The neo-

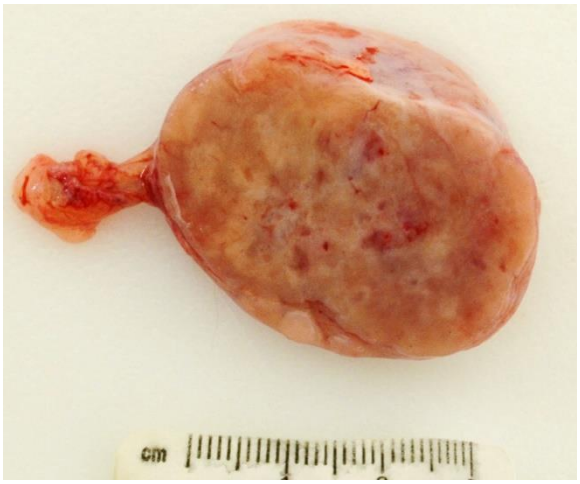

Figure 3-2. Ovary, rhesus macaque. On sectioned surface, the left ovarian neoplasm is mottled tan to red with small scattered areas of central necrosis and hemorrhage, and is contained by a thin fibrous capsule *Photo courtesy of:* Wake Forest School of Medicine, Department of Pathology, Section on Comparative Medicine,www.wakehealth.edu).

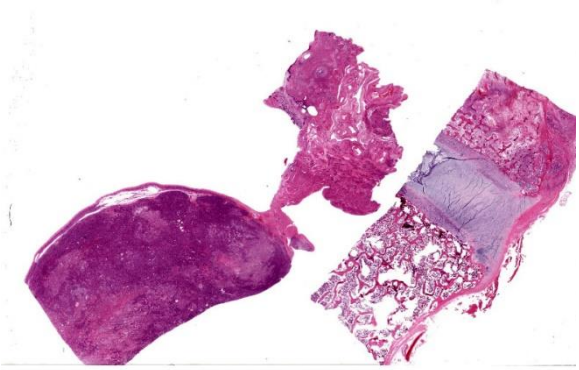

Figure 3-3. Ovary, uterus, vertebra, rhesus macaque. Sections of three organs are submitted for examination. The normal ovarian architecture (bottom left) is effaced by a neoplasm. (HE 4X)

plastic stroma is less pronounced than that in the ovarian lesion. The remaining bony trabeculae have empty lacunae and are unattended by osteoclasts or osteoblasts (necrosis).

Contributor's Morphologic Diagnosis:
Ovarian carcinoma with vertebral and uterine metastases.

Contributor's Comment:
In this case, subsequent histopathologic exam revealed a similar smaller neoplasm to that described above in the contralateral ovary. Ovarian carcinoma is a rarely reported neoplasm in this species,[7] and domestic animals in general.[5] In humans, metastases from the ovary to bone is rare, and in one survey of 1,481 cases of stage IV ovarian carcinoma, only 32 (3.2%) had bone metastases.[1] Bilateral carcinomas are reported in approximately 25% of humans with ovarian cancer,[6] and are relatively common in dogs as well.[5] The dense mesenchymal component of the primary tumor in this case was striking and the morphology did not fit into the common subtypes of ovarian carcinomas described in domestic animals and humans, IE: papillary, cystic, serous, endometrioid, clear cell or mucinous.[5]

In humans, differentiating primary ovarian carcinoma from metastatic intestinal carcinoma often proves challenging, as the ovaries are common metastatic sites. Metastatic intestinal carcinomas often histologically mimic ovarian carcinomas in humans, and while identifying the typical features of metastatic neoplasms may prove useful, none are considered highly specific.[3] Considering the history of intestinal adenocarcinoma in this animal, ruling-out intestinal adenocarcinoma was salient in this case. At necropsy, the entire intestinal tract was closely examined for evidence of recurrence but no gross or histologic intestinal neoplastic lesions were discovered.

Historically, the immunohistochemical (IHC) panel used to differentiate primary ovarian carcinoma from metastatic intestinal carcinoma included cytokeratin-7, cytokeratin-20, carcinoembryonic antigen (CEA) and cancer antigen-125, summarized in Table 1.[3] However, more recent studies have shown that tumors with a mucinous subtype further complicate diagnostics.[4] The contributors determined

Table 1:

Antibodies	Primary ovarian carcinoma	Metastatic intestinal carcinoma	Primary ovarian carcinoma (mucinous)
CK 7	+	-/+	+/-
CK 20	-	+	-/+
CEA	-	+	-/+
CA 125	+	-/+	+/-

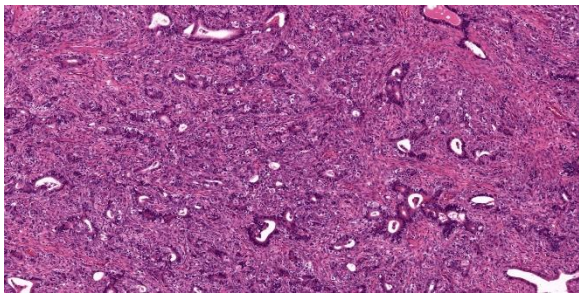

Figure 3-4. Ovary, rhesus macaque. Ovarian architecture is effaced by an epithelial neoplasm in which the neoplastic cells form well-defined tubules and acini on a moderately dense fibrous stroma. (HE, 110X)

that this his particular neoplasm was not mucinous.

Unfortunately the COVID-19 global pandemic precluded the completion of an IHC panel for this case prior to the Wednesday Slide Conference submission deadline, but will be performed at some stage and the results will be submitted.

Contributing Institution:
Wake Forest School of Medicine
Department of Pathology, Section on Comparative Medicine
Medical Center Boulevard, Winston-Salem, NC 27157
www.wakehealth.edu

JPC Diagnoses:
1. Ovary, uterus: Adenocarcinoma.
2. Vertebral body: Metastatic adenocarcinoma.

JPC Comment:
Dr. Eckhaus noted that in his experience, primary ovarian neoplasms are very rare in non-human primates – in his review of nearly 20,000 cases across almost 40 years at the NIH, he noted 4 total cases of ovarian neoplasia that were all benign (three adenomas and one granulosa cell tumor).

Tissue identification proved to be a bit of a problem for participants, as no normal ovarian tissue was present on the slide, and the orientation of the uterus is somewhat problematic. Intestinal adenocarcinoma, a very common malignancy in rhesus macaques, was favored by many participants given the formation of tubules and acini within the mass. This proved to be an important rule out for this case given this animal's previous history (which participants were not privy to before the case discussion). We completed the immunohistochemical panel suggested by the contributor in Table 1 with the exception of CA 125 which was not available in our lab. Neoplastic cells demonstrate strong cytoplasmic immunopositivity for AE1/AE3, consistent with an epithelial neoplasm. CEA, CK 7, and CK 20 were all immunonegative, which likely excludes a metastatic intestinal carcinoma. Other potential differentials that we considered are a fimbrial (oviductal) adenocarcinoma and uterine adenocarcinoma given the proximity of these neoplastic cells to the uterus (figure 3-6). Ultimately, as ovary cannot be identified as a primary site on the submitted HE, we prefer a morphologic diagnosis of carcinoma within the ovary to ovarian carcinoma in this case. (We do believe that the contributors correctly identified ovary at necropsy; it is simply the difficult of making this identification on the

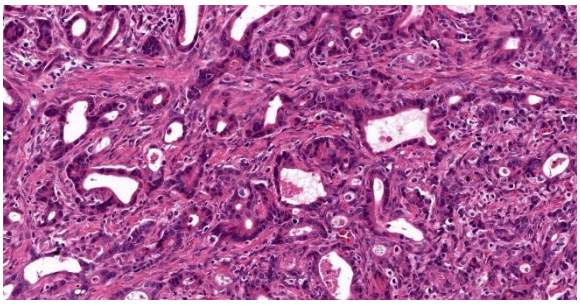

Figure 3-5. Ovary, rhesus macaque. High magnification of neoplastic cells. (HE, 292X)

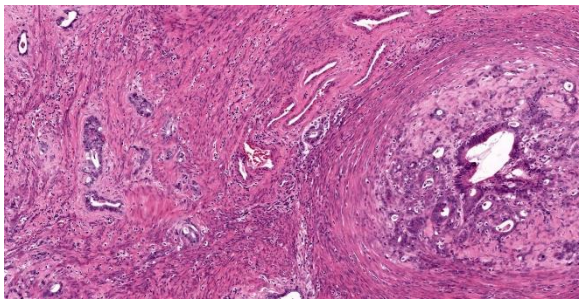

Figure 3-6. Uterus, rhesus macaque. Neoplastic cells infiltrated the mural smooth muscle of the uterus. (HE, 110X)

submitted HE slides which makes us reticent to go "all-in" on this histologic diagnosis as well. Conference participants found the dramatic vertebral changes easier to interpret for this case (figure 3-7).

Although ovarian epithelial neoplasms are rare in NHPs, they are common in human females.[8] Metastases to bone are rarely reported in humans, with a prevalence of approximately 1% in a large cohort study of over 32,000 ovarian carcinoma patients.[8] The frequency of ovarian neoplasms is companion animals is likely adversely impacted by the common practice of ovariohysterectomy, although malignant epithelial tumors do occur in female dogs. In a recent retrospective, 4 out of 18 dogs with malignant ovarian tumors had metastasis to regional lymph nodes, the lung, and/or the brain – bone is not a common site for metastasis in the dog, either.[2]

References:

1. Deng K, Yang C, Tan Q, et al. Sites of distant metastases and overall survival in ovarian cancer: A study of 1481 patients. *Gynecol Oncol*. 2018;150**:** 460-465.
2. Goto S, Iwasaki R, Sakai H, Mori T. A retrospective analysis on the outcome of 18 dogs with malignant ovarian tumours. *Vet Comp Onco*l. 2021; 19: 442–450.
3. Kir G, Gurbuz A, Karateke A, Kir M. Clinicopathologic and immunohistochemical profile of ovarian metastases from colorectal carcinoma. *World J Gastrointest Surg*. 2010;2**:** 109-116.
4. Lin X, Lindner JL, Silverman JF, Liu Y. Intestinal type and endocervical-like ovarian mucinous neoplasms are immunophenotypically distinct entities. *Appl Immunohistochem Mol Morphol*. 2008;16**:** 453-458.
5. Meuten DJ. *Tumors in domestic animals*, Fifth edition. ed. pp. viii, 989 pages. Ames, Iowa: Wiley/Blackwell; 2017.
6. Micci F, Haugom L, Ahlquist T, et al. Tumor spreading to the contralateral ovary in bilateral ovarian carcinoma is a late event in clonal evolution. *J Oncol*. 2010;2010**:** 646340.
7. Simmons HA, Mattison JA. The incidence of spontaneous neoplasia in two populations of captive rhesus macaques (Macaca mulatta). *Antioxid Redox Signal*. 2011;14**:** 221-227.
8. Zhang C, Guo X, Peltzer K, et al. The prevalence, associated factors for bone metastases development and prognosis in newly diagnosed ovarian cancer: a large population based real-world study. *J Cancer*. 2019 Jun 2;10(14):3133-3139.

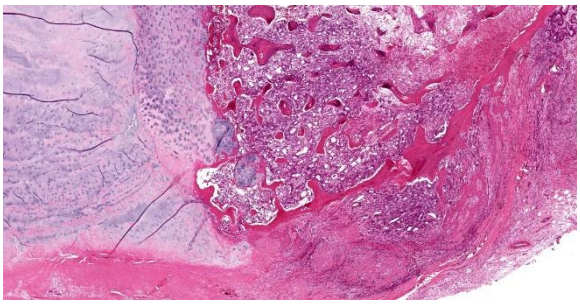

Figure 3-7. Vertebra, rhesus macaque. There is a metastatic focus within the vertebral body, resulting in loss of both trabecular and lamellar bone and resulting in a focus of periosteal new bone growth over the neoplasm. (HE, 27X)

CASE IV:

Signalment:
Adult, male African Green monkey (Chlorocebus sabeus).

History:
An adult male African green monkey had been wild caught on St. Kitts and arrived in quarantine in Maryland in November 2023 with limited clinical history prior available to September 2023.

He had four physical exams during September and October 2023 at the holding/shipping facility on St. Kitts which were unremarkable. He had received four doses of ivermectin and two doses of Drontal plus at the holding facility.

During the initial quarantine examination in November, he was noted to have mild bradycardia and a superficial injury on his distal tail. His appetite was reduced for biscuits, but he was interested in some fruit. On the technician recheck several days later he was noted to fall off his perch when stimulated. During the veterinary cage-side exam, he was bright, alert, and responsive. His head consistently tilted to the right during the exam. When gently stimulated he readily got off the perch and immediately circled to the right 1-2 times. This circling was repeatable and consistent to the right. No ataxia or nystagmus was appreciated. He was started on cerenia and appetite monitoring. A behavior consult was unremarkable. His reduced appetite continued through weekend. He was noted to have a possible right sided-tongue deviation on December 2nd but otherwise clinical signs remained relatively static (R sided head tilt w/right sided circling). Endoparasitology was positive for *Schistosoma mansoni* ova by fecal floatation exam on December 4th. Euthanasia was elected due to poor prognosis, and he was submitted for necropsy two days later.

Figure 4-1. Cerebrum, African green monkey. One section of cerebrum is submitted for examination. at subgross magnification, there is multifocal hypercellularity within the meninges and Virchow-Robin's spaces. (HE, 5X)

Gross Pathology:
A male African Green monkey was submitted following euthanasia with a history of a positive finding of *Schistosoma mansoni* on recent fecal endoparasite examination. The monkey was well-hydrated, well-muscled and contained adequate body fat. On examination of the chest cavity, there were mild adhesions between the left caudal lung lobe and the thoracic wall. The lung lobes were congested with no evidence of pneumonia and these lobes floated in formalin. The heart, kidneys, liver, gallbladder, spleen, pancreas and lymph nodes appeared normal. The stomach contained a moderate amount of ingesta and formed content was present in the colon. No abnormalities were noted involving the mesentery or mesenteric lymph nodes. The urinary bladder and testes appeared normal. The brain appeared grossly normal.

Laboratory Results:
Endoparasitology was performed and was positive for *Schistosoma mansoni* ova and Entamoeba sp.

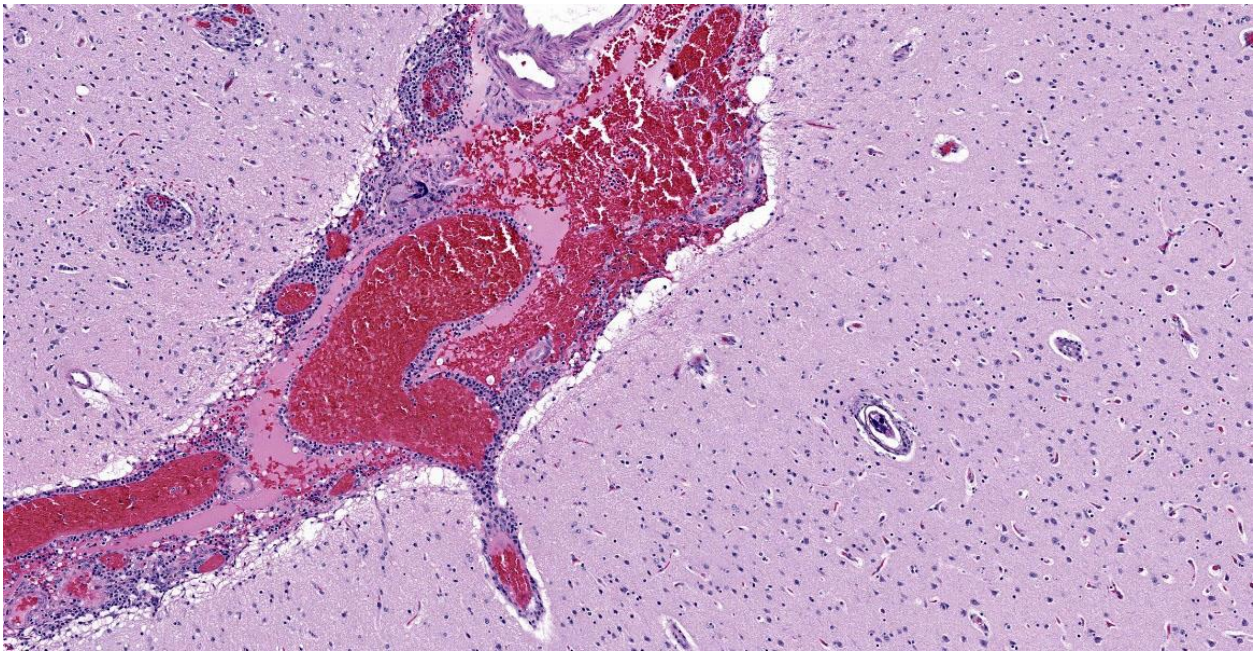

Figure 4-2. Cerebrum, African green monkey. Meninges and Virchow-Robins spaces are expanded by numerous macrophages, lymphocytes and plasma cells as well as hemorrhage. Within the parenchyma, there are scattered microgranulomas which are centered on schistosome eggs. (HE, 83X)

Microscopic Description:
Histopathology revealed multiple small granulomas throughout the hepatic parenchyma containing Schistosoma ova. A solitary granuloma containing a Schistosoma ova was noted in one of several lung sections. Mild nonuppurative pulmonary perivasculitis was present. Examination of sections of cerebrum, cerebellum, medulla and spinal cord revealed meningoencephalitis with multiple granulomas containing Schistosoma ova in the cerebrum, cerebellum and medulla. Sections of the middle/inner ears appeared normal. No other histologic lesions were noted.

Contributor's Morphologic Diagnosis:
Cerebrum: encephalitis, granulomatous, multifocal containing *Schistosoma mansoni* ova.

Contributor's Comment:
Schistosomiasis (also known as bilharziasis) is named after Theodor Bilharz, a German surgeon who discovered *S. haematobium* in 1851.

Schistosomiasis is a major problem worldwide with over 230 million people infected and approximately 200,000 deaths annually. It has been reported in over 52 countries primarily affecting the Eastern Mediterranean, South American, Africa, and the Caribbean.[11] The cause is a blood borne trematode, *Schistosoma sp*. with three primary species – *S. mansoni*, *S. japonicum* and *S. haematobium*. Laboratory identification commonly relies on identification of parasitic eggs in fecal material. The morphology of the eggs is characteristic for each species with *S. mansoni* having a distinct lateral spine.

The life cycle of *Schistosoma mansoni* is complex and indirect, requiring infection of an intermediate freshwater *Biomphalaria* snail.

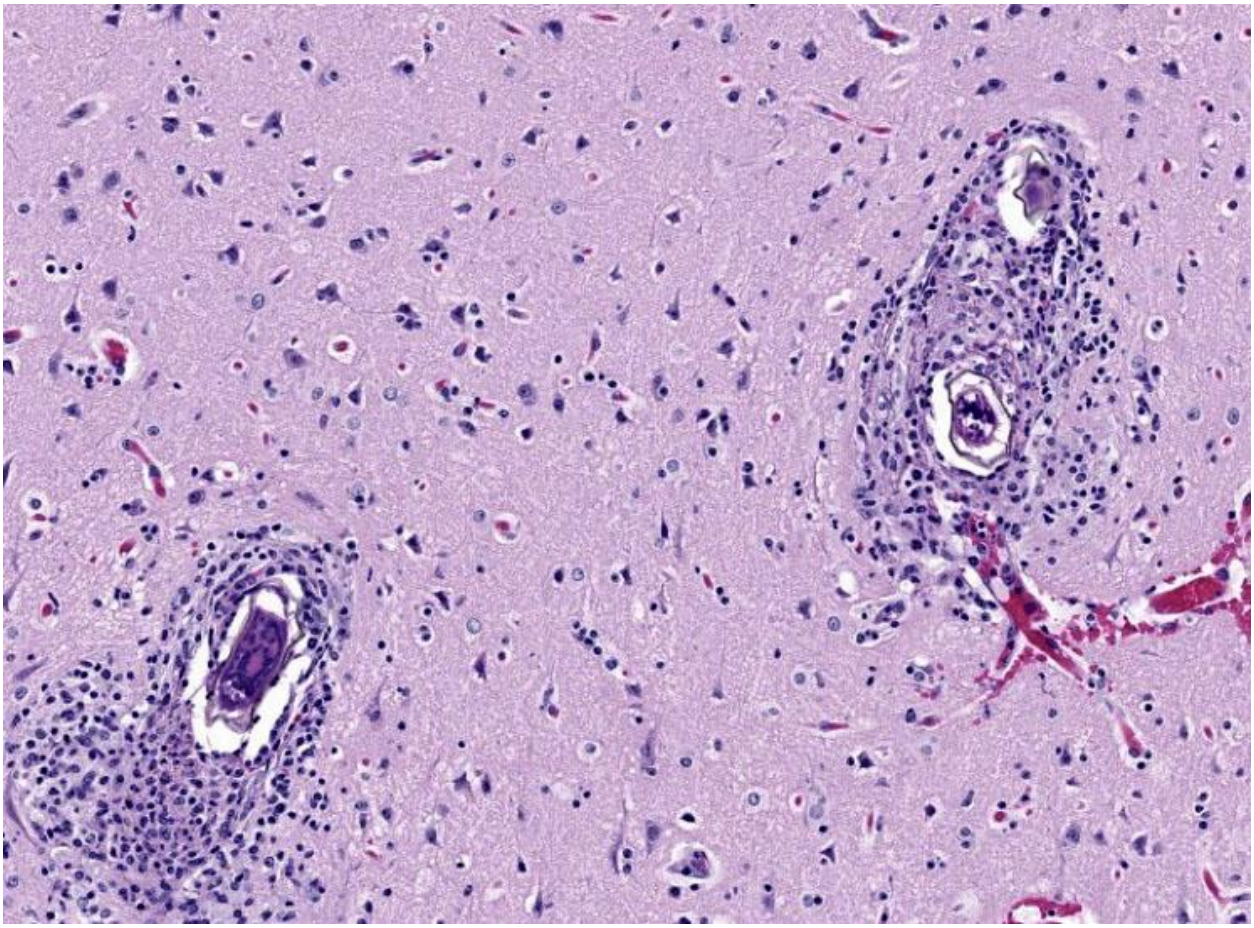

Figure 4-3. Cerebrum, African green monkey. Higher magnification of microgranulomas containing schistosome eggs. Eggs are surrounded by a yellow-brine hyaline shell and often contain a miracidium. (HE, 151X)

Cercariae are released after 4-6 weeks from infected snails and may survive up to 72 hours.

Cercariae attach to the skin of definitive hosts and penetrate the skin to enter dermal vessels, ultimately reaching the pulmonary and hepatic vasculature with maturation to adults in mesenteric veins. Male and female adults maintain a copulatory union in the mesenteric vessels. Ova travel to the lumen of the intestinal tract, are shed in feces, and hatch to free swimming cercariae which can survive up to 3 weeks before infecting appropriate snails to complete the life cycle.[11]

Schistosomiasis is a significant zoonotic disease. While humans are the definitive host, other vertebrate animals may play a significant role with the ability to transmit the agent within the environment. Wild rodents, domesticated animals, and nonhuman primates can serve as additional hosts for this infection.[2] Nonhuman primates including African green monkeys, patas monkeys, chimpanzees, and baboons have become infected with *Schistosoma mansoni* in a number of different African and Caribbean countries.[5] In 2019, an African green monkey from St. Kitts tested positive on fecal examination for *S. mansoni*. This was the first positive report in an African green monkey on St. Kitts after the island was declared negative for the presence of *S. mansoni* during the preceding 50 years.[6]

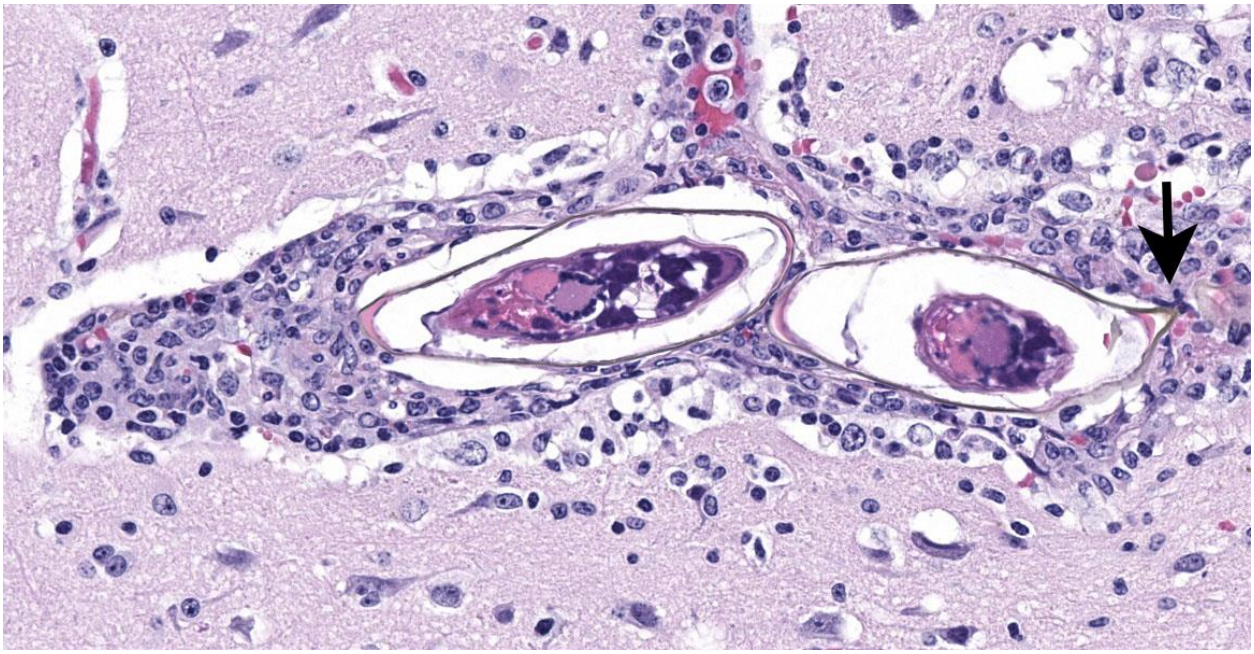

Figure 4-4. Cerebrum, African green monkey. High magnification of schistosome eggs. A lateral spine is present on one (arrow).

Diagnosis of *Schistosoma mansoni* relies primarily on endoparasitologic examination of fecal matter for shed ova. Due to possible discontinuous and insufficient shedding of ova

fecal examination should be conducted analyzing several samples collected on alternate days. PCR analyses for *Schistosoma* ITS-2 DNA sequence can be employed and indirect serologic assays are also available. Clinical findings may include fever, hepatosplenomegaly, eosinophilia and possibly CNS

signs.[8] The treatment of choice for schistosomiasis is praziquantel which targets adult parasites. The drug induces paralysis of the adult parasites which detach from vessel walls allowing the ability of host's immune responses to target the parasites. Additional drug therapies and several vaccines are currently in development.[8]

Morbidity is primarily due to the significant antigenicity of the circulating ova which may reach a variety of organs/tissues including the liver, spleen, lung, intestinal tract, testes, epididymis, prostate, uterus, eye, brain and spinal cord.[4] The inflammatory cell reaction in schistosomiasis is principally due to the intense granulomatous reaction to the dispersed ova. Ova become surrounded by T and B lymphocytes, epithelioid macrophages, foreign body type giant cells, eosinophils, and limited numbers of neutrophils. Chronic infection results in the development of fibrosis with collagen deposition (1). Numbers of studies of the granulomas have identified various lymphocytic subsets including B cells, Th17 cells and Treg cells, as well as various cytokines, chemokines and vascular endothelial factor.[3]

Neurologic involvement of *Schistosoma mansoni* infection can affect both the brain and spinal cord. The development of CNS signs depends on the relative numbers of ova within the brain and spinal cord and the severity of the accompanying inflammatory cell reaction. Clinical signs may include ataxia, nystagmus, visual impairment, and seizures. Vascular embolization of individual eggs is the most common mode for CNS involvement.[7]

Contributing Institution:
Diagnostic and Research Services Branch, Division of Veterinary Resources, National Institutes of Health, Bethesda, Maryland

JPC Diagnosis:
Cerebrum: Meningoencephalitis, granulomatous and eosinophilic, multifocal to coalescing, moderate with perivascular schistosome eggs.

JPC Comment:
The final case of this conference features a short description and an interesting backstory. Dr. Eckhaus actually submitted this case and was intently interested in the development of this lesion given the lack of overt pathology at necropsy. From subgross (figure 4-1), perivascular basophilia is indicative of the inflammatory response elicited by circulating schistosome ova within and extending from blood vessels (figure 4-2). Recognizing that these granulomas are centered on blood vessels and the lack of other life stages in section (larva or adult) is helpful for ruling out other metazoan parasites as the cause of the meningoencephalitis in this case. We were able to speciate the schistosome as *S. mansoni* by the distinct lateral spine (figure 4-4, arrow) which *S. japonicum* and *S. haematobium* lack. Conference participants briefly reviewed other sections of this case provided by Dr. Eckhaus, but were unable to identify adult schistosomes in section. As this animal was dewormed with praziquantel multiple times before developing overt clinical disease, it is likely that deworming likely removed adult trematodes from the vessels, but had no effect on the eggs already present within the bloodstream or perivascular tissues.

Finally, we elaborate further on the connection between granulomas and the life cycle of *Schistosoma*.[9,10] The ova of *S. mansoni* are metabolically active and highly antigenic, a combination that allows them to recruit inflammatory cells as a means to migrate from blood vessels into the lumen of the gut for excretion.[9,10] The ova secretes factors to potentiate attachment to the endothelium as well as bias the immune response of the host towards a Type 2 (Th2) response with marked increases in IL-4, -5, and -13.[9,10] Interestingly, these same proteins can also upregulate cellular adhesion molecules such as ICAM-1 on endothelial cells and increase recruitment of inflammatory cells to the nascent granuloma. The exact mechanism of movement through the extracellular milieu is unclear, though the role of M2 macrophages and matrix metalloprotease activity is likely.[9] Fibrosis induced by the M2 phenotype may also partially protect ova from eosinophils and basophils.[10] In addition, ova also have the ability to increase plasminogen activation which serves to clear fibrin and fibronectin alike. Likewise, how exactly the ova 'eggs-its'[9] out of this granuloma to enter the gut lumen has not been described, though interactions between the ova, gut microbiome, and macrophages are a possibility. Interestingly, humans and mice models with T-cell deficiencies shed fewer ova in their feces, highlighting the role of Th2 polarity in the life cycle of this parasite.

Finally, the timing of this immune relationship is key as immature ova do not recruit inflammatory cells and evade (initially) granuloma formation.[10] Additionally, schistosome ova only undergo development within the host. Together, this may be adaptive in that it ensures viable, developed miracidia are ready to be released to continue the life cycle.

References:

1. Carvalho OA. Mansonic neuroschistosomiasis. *Arq Neuropsiquiatr*. 2013 Sep;71(9B):714-6.
2. Modena CM, dos Santos Lima W, Coelho PM. Wild and domesticated animals as

reservoirs of Schistosomiasis mansoni in Brazil. *Acta Trop*. 2008 Nov-Dec;108(2-3):242-4.
3. Giorgio S, Gallo-Francisco PH, Roque GAS, Flóro E, Silva M, Granlulomas in parasitic diseases: the good and the bad. *Parasitol Res*. 2020 Oct;119(10):3165-3180.
4. Gryseels B. Schistosomiasis. *Infectious Disease Clinics of North America*; June 2012, 383-397.
5. Kebede T, Bech N, Allienne JF, Olivier R, Erko B, Boissier. Genetic evidence for the role of non-human primates as reservoir hosts for human schistosomiasis._*J.PLoS Negl Trop Dis*. 2020 Sep 8;14.
6. Ketzis JK, Lejeune M, Branford I, Beierschmitt A, Willingham AL. Identification of *Schistosoma mansoni* Infection in a Nonhuman Primate from St. Kitts More than 50 Years after Interruption of Human Transmission. *Trop Med Hyg*. 2020;103(6):2278-2281.
7. Llanwarne F, Helmby H. Granuloma formation and tissue pathology in Schistosoma japonicum versus Schistosoma mansoni infections. Parasite Immunol. 2021 Feb;43(2):e12778.
8. Ponzo E, Midiri A, Manno A, Pastorello M, Biondo C, Mancuso G. Insights into the epidemiology, pathogenesis, and differential diagnosis of schistosomiasis. Eur J Microbiol Immunol (Bp). 2024 Mar 18;14(2):86-96.
9. Schwartz C, Fallon PG. Schistosoma "Eggs-Iting" the Host: Granuloma Formation and Egg Excretion. *Front Immunol*. 2018 Oct 29;9:2492.
10. Takaki KK, Rinaldi G, Berriman M, Pagán AJ, Ramakrishnan L. Schistosoma mansoni Eggs Modulate the Timing of Granuloma Formation to Promote Transmission. *Cell Host Microbe*. 2021 Jan 13;29(1):58-67.
11. Verjee MA. Schistosomiasis: still a cause of significant morbidity and mortality. Res *Rep Trop Med*. 2019;10:153–63.